Studia Quaternaria, vol. 43 (2026): 1–16
DOI: 10.24425/sq.2026.158728

PARTICLE SIZE DISTRIBUTION IN AGRICULTURAL HILLSLOPE SOIL: CASE OF MECHTAT KEF LAATATFA, OULED HAMLA (NE ALGERIA), USING COMPOSITIONAL AND MULTIVARIATE ANALYSIS

Chams Abid[1,2*], Rabah Zedam[1], Hassan Taib[3,4], El Hadi Mazouz[1,2], Rihab Hadji[4,5], Marwa Benslama[1,2]

[1] *Department of Geology, Faculty of Earth Sciences and Architecture, Larbi Ben M'hidi University, Oum El Bouaghi, Algeria; e-mails: (CA) chams.abid@univ-oeb.dz, (ZR) zedam.rabah@univ-oeb.dz, (EHM) emazouz@univ-oeb.dz, (MB) Benslama.marwa@univ-oeb.dz*

[2] *Laboratory of Natural Resources and Management of Sensitive, Larbi Ben M'hidi University, Oum El Bouaghi, Algeria*

[3] *Department of Geological Sciences, Faculty of Earth Sciences, Geography and Regional Planning, University Frères Mentouri Constantine 1, P.O. Box, 325 Ain El Bey Way, Constantine 25017, Algeria; (HT) hacentaib68@gmail.com*

[4] *Laboratory of Applied Research in Engineering Geology, Geotechnics, Water Sciences, and Environment, Ferhat Abbas University, El Bez, Setif, 19137, Algeria; email: (RH) hadjirihab@yahoo.fr*

[5] *Department of Earth Sciences, Institute of Architecture and Earth Sciences, Ferhat Abbas University, El Bez, Setif, 19000, Algeria*

** corresponding author*

Abstract:
This study examines the spatial variability of soil particle-size distribution (PSD) along an agricultural hillslope at Mechtat Kef Laatatfa (Ouled Hamla, northeastern Algeria). The vertical and lateral organization of PSDs is investigated in relation to morphological setting, hydroclimatic conditions, and lithological context, which are considered the primary controls on sediment redistribution along the slope. The study aims to assess the added value of combining compositional and multivariate analytical approaches for interpreting particle-size variability in hillslope soils. Soil samples were collected from exposed horizons of three representative soil profiles and analysed using dry-sieving granulometry. Compositional data analysis (CoDA), principal component analysis (PCA), and end-member modelling analysis (EMMA) were jointly applied to disentangle granulometric patterns and transport-related processes. The results show that PSD accumulation is primarily governed by parent material erosion and slope gradient, with subsequent modification by size-selective sorting during downslope transport. A marked reduction in granulometric variability is observed from upslope to downslope positions, reflecting a systematic transition from coarse- to fine-dominated textures along the geomorphological gradient. By integrating compositional and multivariate techniques, this study provides a more robust and process-oriented interpretation of soil textural patterns along agricultural hillslopes, highlighting their relevance for understanding sediment redistribution under cultivated conditions.

Key words: Ouled Hamla, particle-size distribution (PSD), compositional data analysis (CoDA), principal component analysis (PCA), end-member modelling analysis (EMMA).

Manuscript received January 2026, accepted 8 February 2026

INTRODUCTION

External geodynamics of the Earth's crust plays a fundamental role in the transformation of rocks into soils through its close interaction with surface geological, environmental and anthropogenic processes (Dahoua *et al.*, 2017; Zerzour *et al.*, 2020, 2021; Saadoun *et al.*, 2022; Taib *et al.* 2024a, b). Among exogenic agents, water acts as the primary driver of both physical disintegration and chemical weathering of rocks (Arif *et al.* 2024; Ladjel *et al.*, 2024). Through its mechanical action (via runoff, infiltration, freeze-thaw cycles, and sediment transport) water fragments rock materials, while chemically it promotes dissolution, hydrolysis, oxidation, and carbonation reactions. These combined processes lead to the progressive development of weathered materials, characterized by selective enrichment or depletion of chemical elements (Chibani *et al.*, 2024; Hamed *et al.*, 2024). The subsequent evolution of these materials is governed by the combined influence of climate, topography, biological activity, and time (Ncibi *et al.* 2022; Benmarce *et al.* 2023). Together, these interacting mechanisms form the basis of pedogenesis, positioning soil as a dynamic interface linking the lithosphere, hydrosphere, atmosphere, and biosphere.

Soil particle size distribution (PSD) is a key physical attribute that encapsulates both the lithological characteristics of the parent material and the intensity of sedimentary processes (erosion and transport) to which the soil has been subjected. In landscapes marked by strong relief and mechanically weak or easily weathered parent rocks, soil formation is spatially differentiated between zones of particle production and zones of particle accumulation, leading to pronounced textural contrasts along hillslopes (Sommer and Schlichting, 1997). These contrasts are further shaped by climatic conditions and biological activity, which jointly regulate weathering intensity, translocation processes, and structural organization within soil profiles over time (Chen *et al.*, 1997; McKenzie and Ryan, 1999; Buol *et al.*, 2011).

In sloping environments, particle size dynamics acquire particular significance because slope position exerts a primary control on erosion, leaching, transport, and depositional processes. The interplay of these mechanisms governs both the vertical differentiation of soil horizons and the lateral redistribution of fine and coarse fractions along the slope continuum (Tancredi *et al.*, 2022). In agricultural contexts, PSD influences a wide range of soil functions, including hydraulic conductivity, organic matter stabilization, nutrient retention, and root development, while also determining soil vulnerability to erosion, moisture stress, and long-term degradation (Chi *et al.*, 2021). Consequently, a refined and quantitative characterization of PSD (beyond conventional textural classes) is essential for advancing understanding of soil-environment interactions and land sustainability (Wang *et al.*, 2023).

However, particle size analysis remains underutilized. Most studies have relied on characterising soil texture in broad categories (sand/silt/clay), but these descriptions often obscure subtle vertical transitions between horizons (Han *et al.*, 2025). Studies examining particle size distribution have relied on traditional sedimentological indicators such as sorting, skewness, Kurtosis (Folk and Ward, 1957).

Only a limited number of studies have applied compositional data analysis (CoDA) approaches to soil particle-size distribution (PSD) data, despite the fact that particle-size fractions are inherently constrained to a constant sum and therefore require a statistically coherent analytical framework (Filzmoser and Hron, 2009; Buccianti, 2013). Moreover, vertical granulometric evolution across multiple soil profiles positioned along hillslopes has rarely been examined, even though geomorphological studies clearly demonstrate that slope position exerts a strong control on sediment supply, erosion intensity, illuviation, and overall pedogenic development (Canfield *et al.*, 2001; Anderson R.S. and Anderson S.P, 2010; Sklar *et al.*, 2017).

In agricultural landscapes, variations in slope gradient and relative position (upslope-midslope-downslope) regulate the balance between sedimentary redistribution and in situ soil-forming processes, leaving characteristic signatures in the vertical texture of soil horizons that can be captured by particle-size data. High-resolution PSD measurements based on multiple sieve fractions provide a more detailed representation of internal soil structure than conventional textural classifications. Because particle-size data are compositional in nature, their analysis requires statistical methods that account for relative information and closure constraints. The Aitchison framework offers such an approach and has been shown to be more appropriate than classical Euclidean-based methods for analysing soil PSD data (Aitchison, 1986; Filzmoser *et al.*, 2009; Pawlowsky-Glahn; Egozcue, 2020). Log-ratio transformations, including centered log-ratio (CLR) and isometric log-ratio (ILR), provide a consistent basis for applying multivariate statistical techniques to compositional soil data (Aitchison, 1986; Egozcue *et al.*, 2003).

Against this background, the present study investigates the vertical and lateral evolution of soil particle size across three soil profiles (P2, P4, and P5) distributed along a hillslope in the Mechtat Kef Laatatfa area. The specific objectives are to: (i) characterize the vertical grain size distribution within successive horizons (An–A0) for each profile; (ii) compare vertical granulometric trends among profiles to identify systematic topographic controls; (iii) evaluate the performance of compositional and multivariate statistical approaches in interpreting PSD; and (iv) explore relationships between particle size distribution and topographic attributes.

Methodologically, the study integrates CoDa techniques with principal component analysis (PCA), Aitchison distance metrics, variation matrices, and end-member modeling analysis (EMMA). This combined approach overcomes key limitations of traditional particle size descriptors and provides a more coherent and process-oriented interpretation of granulometric evolution. By coupling advanced compositional statistics with detailed particle size measurements, this research contributes to understanding of soil formation and surface dynamics in sloping agricultural landscapes.

GENERAL SETTING

Mechtat Kef Laatatfa is an important rural and agricultural area located within the municipality of Ouled Hamla, approximately 18 km northwest of the city of Ain M'lila, at coordinates 36°07′15″ N and 6°26′01″ E (Fig. 1). The locality of Ouled Hamla is situated at the northern edge of the Saharan Atlas, within the structural domain of the Constantinois Mountains. The study area occupies a transitional zone characterised by Quaternary and Mio-Pliocene cover deposits, bordered by Cretaceous and Paleogene outcrops (Fig. 2).

The lithostratigraphic evolution of Ouled Hamla reflects successive shallow-marine, regressive, and transgressive phases, expressed by alternating carbonates, marls, and detrital deposits (Van de Fliert, 1955; Bär, 1957; Durozoy, 1960; Voute, 1967; Raoult and Fourcade, 1973; Chadi, 2004).

Tectonically, the region shows slight subsidence; its evolution has been marked by three phases: (1) Cretaceous–early Lutetian epi-orogenic movements with stratigraphic gaps; (2) late Lutetian–Tortonian tectonics, including major SW-NE and NW-SE faulting, uplift, and deformation of marls between carbonate blocks; and (3) post-Messinian mild folding (Obert, 1974; Bureau, 1986; Guiraud, 1990; Aris, 1994).

The structural framework comprises tilted Cretaceous monoclines, the Guelaat Ouled Sellem anticline, uplifted compartments, reverse and strike-slip faults, Messinian domes, and Triassic diapirs, reflecting a polyphase tectonic history (Vila, 1980; Kazi-Tani, 1986; Aris, 1994).

Geomorphologically, landforms are closely adjusted to the underlying tectonic and lithological framework, limestone massifs occurring as uplifted blocks with marl levels outcropping in depressions. The mountain boundaries correspond to border faults or hard and soft lithological contacts. The relief is ancient and has been exposed to erosion for a very long time, resulting in the development of cliffs and rounded shapes. The absence of alluvial terraces contrasts with the conglomerate deposits resulting from precipitation, sheet floods, and incised piedmont fans (Bär, 1957; Voute, 1967; Raoult and Fourcade, 1973; Vila, 1980; Bouillin, 1986; Lahondère, 1987; Aris, 1994). Within this geomorphic framework, Quaternary deposits can be subdivided into four units: ancient piedmont alluvium forming stacked fans, recent fine-grained alluvium confined to depressions, valley-floor conglomerates transported by oueds, and slope scree mantling older forma-

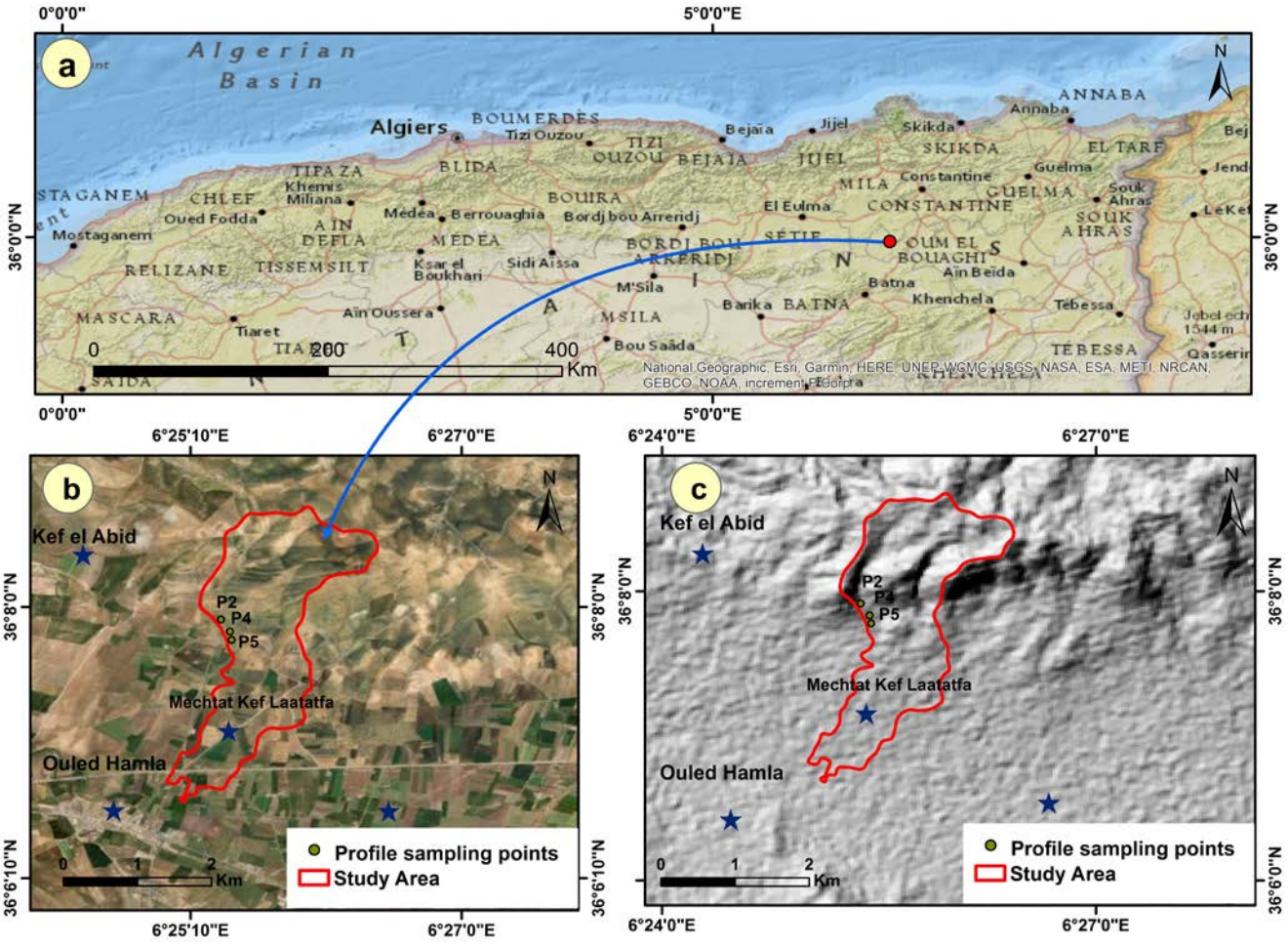

Fig. 1. Location of the study area: (a) regional location within northeastern Algeria; (b) satellite image showing the study area and soil profile sampling points; (c) shaded relief map illustrating topography and profiles distribution.

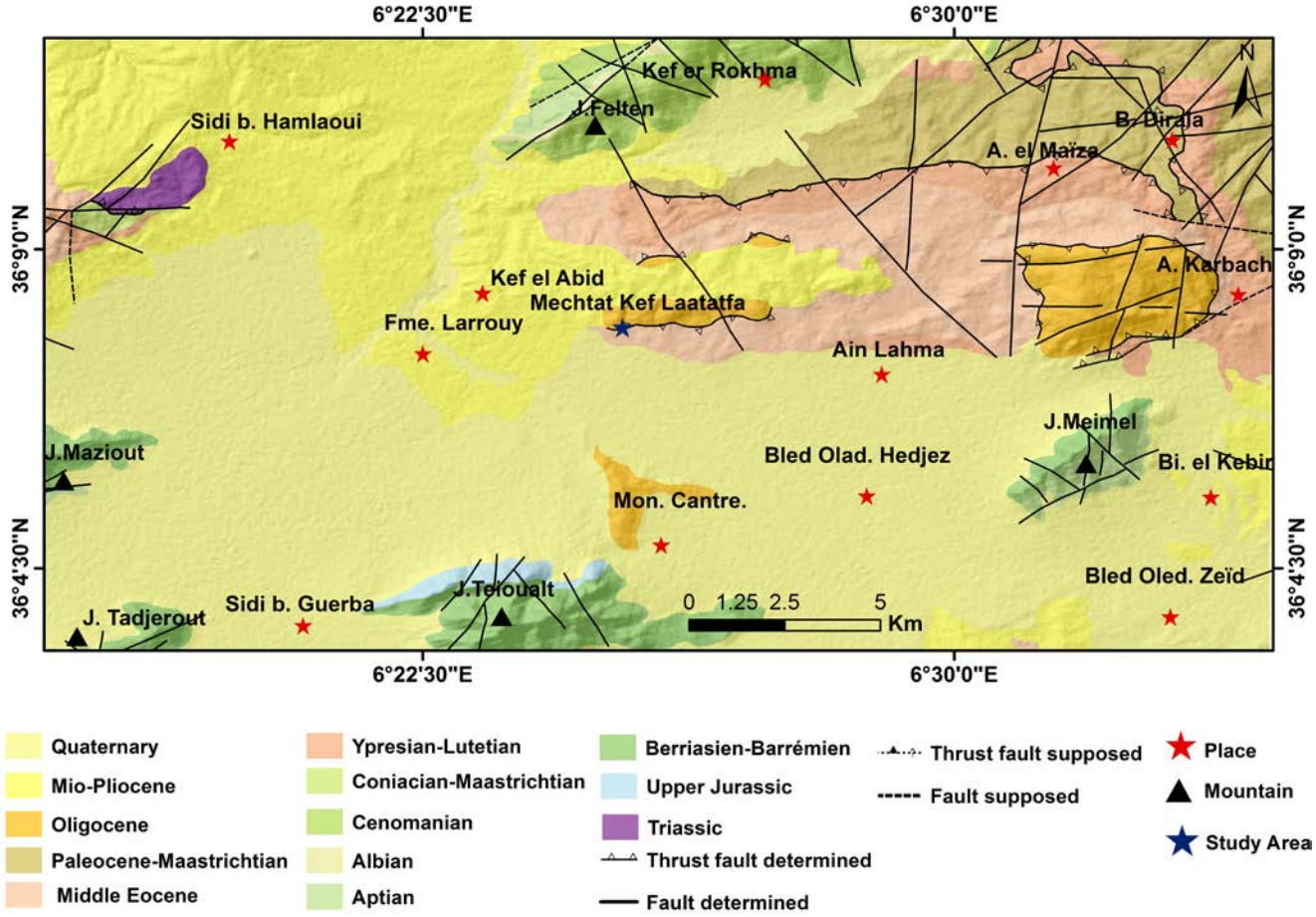

Fig. 2. Schematic geological map of the study area.

tions (Durozoy, 1960; Bureau, 1986; Chadi, 1991; Coiffait, 1992).

MATERIALS AND METHODS

Soil sampling and particle size analysis

Three soil profiles were excavated and sampled along the slope to capture vertical and lateral variations in particle-size distribution. The profiles are located at P2 (36.131913° N, 6.422880° E), P4 (36.130556° N, 6.423889° E), and P5 (36.129538° N, 6.424106° E). Their spatial distribution is shown in Fig. 2, while detailed morphological descriptions of the soil profiles are presented in Fig. 3. Horizon boundaries, thicknesses, and sampling depths (centre of the sample) were identified in situ and are summarized in Table 1.

Within each profile, soil samples were systematically collected from the upper (S1) and lower (S2) portions of each horizon to capture internal textural variability. For horizons exhibiting substantial thickness, additional intermediate samples were taken to improve vertical resolution. All samples were air-dried and subsequently oven-dried to remove residual moisture, then gently disaggregated using a plastic mallet to avoid crushing primary particles.

Grain-size analysis was conducted on 300 g subsamples using dry sieving. Samples were passed through a standardized sieve stack with mesh sizes of 2 mm, 1 mm, 0.500 mm, 0.250 mm, 0.125 mm, and 0.063 mm, with a pan collecting the finest fraction (<0.063 mm). The mass retained on each sieve was weighed, and the relative proportion of each size fraction was calculated as a percentage of the total sample mass.

Table 1. Soil profiles, horizon thickness and depth of samples taken.

Profile	P2									P4								P5										
Horizon	A0		A1		A2		A3			A0		A1		A2		A3		A0		A1		A2		A3				
Thicknesses (cm)	30		29		40		81			40		30		50		65		25		17		26		82				
Sample	S1	S2	S1	S2	S1	S2	S1	S2	S3	S1	S2	S1	S2	S1	S2	S1	S2	S1	S2	S1	S2	S1	S2	S1	S2	S3	S4	S5
Depth (cm)	5	25	35	54	64	94	104	139.5	180	5	35	45	65	75	115	130	170	5	20	30	37	47	62	73	95	110	130	150

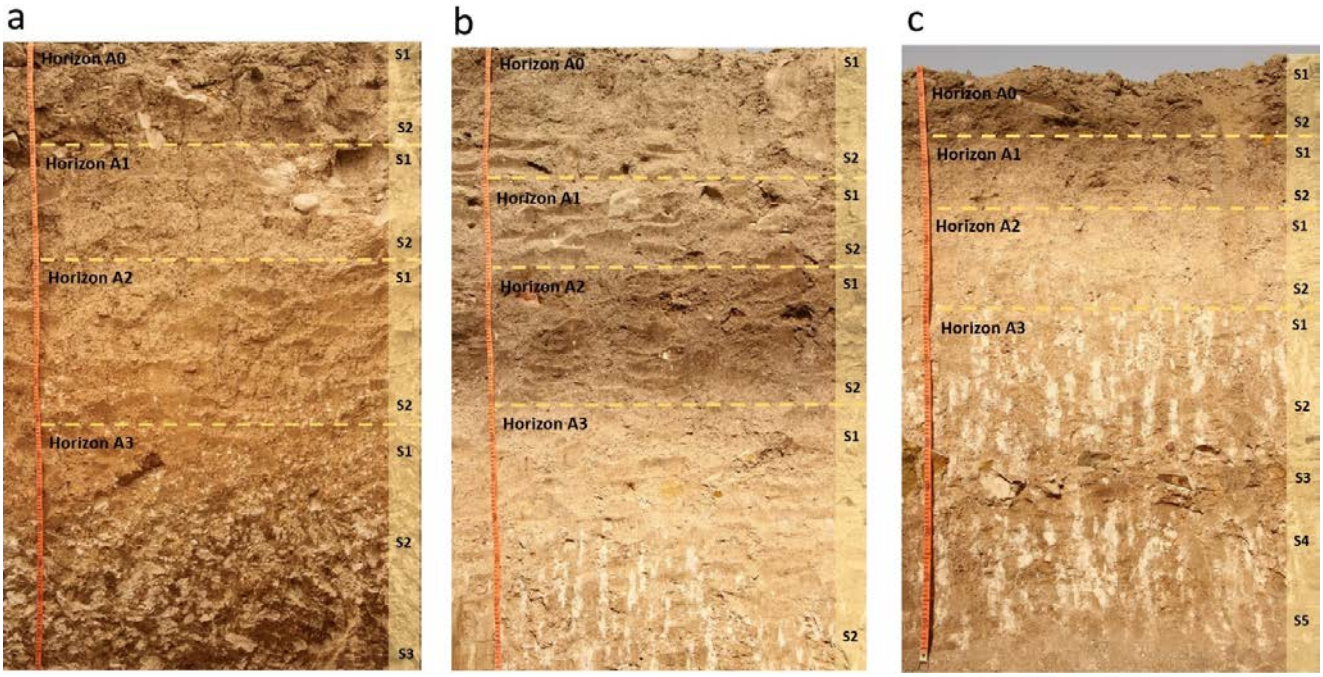

Fig. 3. Photographs of three soil profiles: (a) profile P2, (b) profile P4, and (c) profile P5. with identified horizons and sampling points

Compositional data treatment and log-ratio transformations

Particle-size fractions constitute compositional data, as they represent parts of a whole constrained to a constant sum (100%). Direct statistical analysis of such data can lead to spurious correlations and biased interpretations. To address this issue, all grain-size datasets were analyzed within the framework of compositional data analysis (CoDA) (Aitchison, 1986).

Zero values in the particle-size fractions were treated using multiplicative replacement (Martín-Fernández *et al.*, 2003). Specifically, zeros were replaced by 0.65 × X%, where X% corresponds to the minimum observed fraction percentage within the same horizon and profile. Zero values were rare in the dataset and limited to a single observation. Given their limited occurrence and magnitude, zero replacement had a negligible effect on the overall compositional structure of the data.

This approach preserves relative information while allowing log-ratio transformations.

A sequential binary partition (SBP) scheme was defined to structure the compositional space (Egozcue and Pawlowsky-Glahn, 2005, 2019), as detailed in Table 2. Based on this partition, isometric log-ratio (ilr) transformations were applied to obtain orthonormal coordinates suitable for multivariate statistical analysis (Filzmoser *et al.*, 2009; Hosseinpoor *et al.*, 2015; Egozcue and Pawlowsky-Glahn, 2019). The resulting ilr coordinates, expressed as balances, quantify log-contrasts between two disjoint groups of particle-size fractions:

$$irl\left(\frac{K}{L}\right) = \sqrt{\frac{rs}{r+s}}\ln\left(\frac{g(x^{+})}{g(x^{-})}\right) \qquad \text{Eq. 1}$$

where K and L are the two groups of fractions drawn from the complete set (> 2 mm, 1–2 mm, 0.5–1 mm, 0.25–0.5 mm, 0.125–0.25 mm, 0.063–0.125 mm, <0.063 mm), r and s denote the number of parts in K and L, respectively, and $g(x^{+})$ and $g(x^{-})$ represent the geometric means of the corresponding groups.

This balance expresses the relative dominance of one group of particle-size fractions over another, allowing coarse and fine contrasts within the soil.

For complementary interpretation and visualization of compositional relationships, centered log-ratio (clr) trans-

Table 2. Sequential Binary Partition (SBP) of the particle size fractions.

Balance (in mm)	>2	1–2	0.5–1	0.25–0.5	0.125–0.25	0.063–0.125	<0.06	Interpretation
B1	+1	+1	+1	-1	-1	-1	-1	coarse (≥0.5 mm) (+) / fine (<0.5 mm) (-)
B2	+1	-1	-1	0	0	0	0	very coarse (≥2 mm) (+) / coarse sands (1–2 mm, 0.5–1 mm) (-)
B3	0	0	0	+1	+1	-1	-1	= (0.25–0.5 mm. 0.125–0.25 mm) (+) / (0.063–0.125 mm. <0.063 mm) (-)
B4	0	+1	-1	0	0	0	0	(1–2 mm) (+) / (0.5–1 mm) (-)
B5	0	0	0	+1	-1	0	0	(0.25–0.5 mm) (+) / (0.125–0.25 mm) (-)
B6	0	0	0	0	0	+1	-1	(0.063–0.125 mm) (+) / (< 0.063 mm) (-)

formations were also computed prior to statistical analyses (Aitchison, 1983; Aitchison and Greenacre, 2002).

$$crl\,(x) = \left(\ln \frac{x_1}{g_m(x)}, \ldots\ldots, \ln \frac{x_D}{g_m(x)} \right) \quad \text{Eq. 2}$$

With

$$g_m(x) = (\prod_{i=1}^{D} x_i)^{1/D} \quad \text{Eq. 3}$$

where $g_m(x)$ denotes the geometric mean of the composition.

The clr transformation expresses the relative enrichment or depletion of each particle-size fraction with respect to the overall compositional center, facilitating comparison of PSD patterns across horizons and profiles.

The ilr coordinates used in the PCA were calculated using the same sequential binary partition (SBP) shown in this table, therefore, each SBP balance (B1–B6) corresponds directly to ilr coordinate (ilr1–ilr6).

Multivariate and statistical analyses

Principal Component Analysis (PCA) was applied to the ilr-transformed grain-size data to reduce dimensionality and identify the dominant gradients of textural variability. PCA transforms correlated variables into a reduced number of orthogonal components that retain most of the original information (Syms, 2008; Singh *et al*., 2023). In this study, PCA was used to explore relationships among particle-size fractions, assess their evolution across horizons, and extract the principal components controlling textural organization along the slope.

To evaluate vertical textural trends, scores of the first principal component (PC1) were plotted against depth for each soil profile. This approach provides a quantitative compositional depth profiling, allowing the identification of systematic coarse-to-fine transitions and potential textural discontinuities associated with pedogenic processes or sedimentary inputs (Schaetzl and Anderson, 2005).

Compositional dissimilarities between horizon centroids were quantified using the Aitchison distance (Aitchison, 1982; Filzmoser *et al*., 2009), which provides a robust measure of the magnitude of particle-size transitions within and between profiles. To further assess the behavior of individual fractions, a log-ratio variance matrix was computed and visualized using heatmaps. These matrices highlight pairs of fractions exhibiting high or low variance, thereby identifying size classes most sensitive to pedogenic redistribution or sedimentary reworking along the slope.

Finally, End-Member Modelling Analysis (EMMA) was employed as an exploratory tool to decompose multimodal particle-size distributions into a limited number of statistically robust end-members. The number of end-members (q = 4) was chosen according to the conceptual framework proposed by Dietze *et al.* (2012, 2014), which combines statistical criteria and sedimentological interpretability. Lower q values failed to separate distinct grain size groups, while the four-element solution provides stable and physically meaningful distributions of particle-sizes that can be linked to transport and deposition processes. In this study, EMMA is used to support pattern recognition and comparison among soil profiles by identifying and quantifying distinct particle-size assemblages distributed along the hillslope. (Flemming, 2007; Dietze *et al*., 2012, 2014; Vandenberghe, 2013; van Hateren *et al*., 2018; Dietze *et al*., 2022). Applied in a slope context, this approach provides a process-oriented interpretation of particle-size patterns, linking observed textural variability to sediment sources, transport pathways, and soil-forming processes.

Software

Data processing and statistical analyses were performed in a Python environment using the Anaconda Navigator distribution, with computations executed in the Spyder IDE (version 5.5.1). Data handling and matrix operations were conducted using NumPy (version 1.26.4) and Pandas (version 2.2.2), and figures were produced using Matplotlib (version 3.9.2) with Seaborn (version 0.13.2) used for variation-matrix heatmaps.

Principal component analysis (PCA) was applied to ilr-transformed particle-size data using scikit-learn (version 1.5.1), after mean-centering the ilr coordinates and without additional scaling.

End-member modelling analysis (EMMA) was implemented using a non-negative matrix factorisation (NMF) approach as implemented in scikit-learn. Particle-size fraction data were treated as proportional data and normalised using a closure operation prior to modelling.

RESULTS

Particle size variability

Variability within profiles was investigated using clr-transformed heatmaps (Fig. 4). Since the transformation removes compositional constraints, the heatmaps reveal relative enrichment (positive clr) or depletion (negative clr) of each particle size fraction, relative to the geometric mean of the sample (Pawlowsky-Glahn and Egozcue, 2020). This approach allows the comparison of compositional patterns without closure-induced bias.

In profile P2 (Fig. 4a), coarse fractions (>2 mm) show relatively similar clr values throughout the profile, while intermediate fractions (0.5–2 mm) are more prominent in horizons A2 and A3 and decrease toward the surface. Fine fractions (<0.125 mm) show comparatively lower clr values across the profile. This pattern documents a vertically coherent PSD structure with only modest relative differentiation between horizons. In profile P4 (Fig. 4b), displays markedly higher internal variability, with alternating relative enrichments of intermediate (0.25–0.5 mm) and fine fractions (<0.125 mm) across horizons, indicating marked compositional contrasts within the profile. In pro-

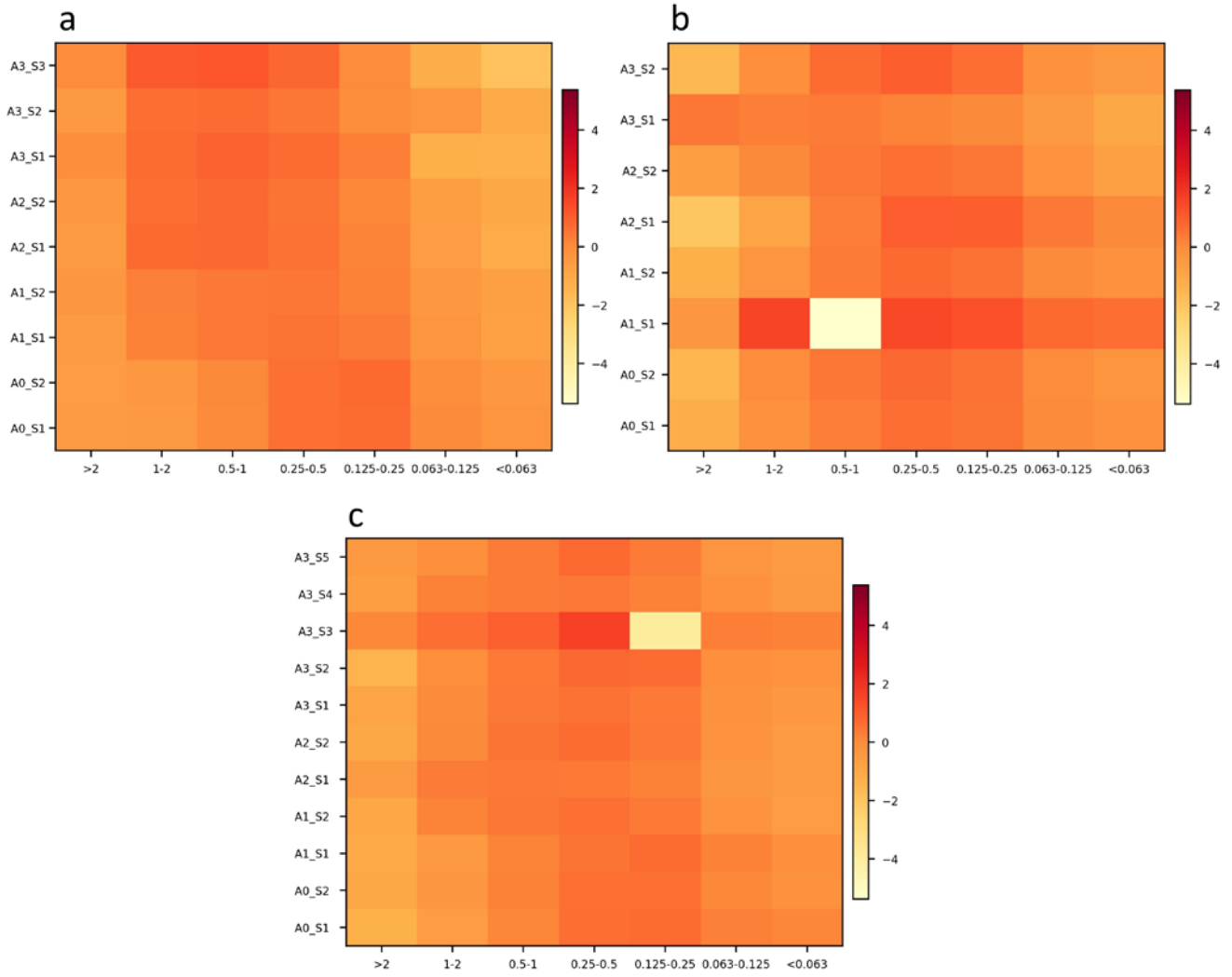

Fig. 4. Clr Heatmaps of particle size fractions of soil profiles, (a) profile P2, (b) profile P4, and (c) profile P5.

file P5 (Fig. 4c) is characterized by a distinct vertical contrast between surface and deep horizons. Deeper horizons (A2–A3) show relative enrichment in fine fractions (<0.125 mm), whereas surface horizons (A0–A1) exhibit a more balanced distribution among particle-size classes. This results in a clear compositional differentiation with depth.

The clr heatmaps indicate systematic vertical compositional contrasts in particle-size distributions along the slope, highlighting differences in the internal structure of particles among profiles.

Vertical compositional structure: PCA and evolution of PC1_depth

Principal Component Analysis (PCA) was applied to synthesize the vertical evolution of particle-size composition within each profile (Fig. 2a–c). The first principal component (PC1) accounts for the dominant share of variance (83.3–88.9%) and represents a continuous gradient from coarse to fine fractions. In contrast, PC2 explains a smaller

Table 3. ilr-PCA loadings for the principal components PC1 and PC2 for profiles P2, P4 and P5.

ilr balance	Profile	PC1	PC2
ilr1	P2	+0.865	-0.081
ilr2		-0.246	+0.457
ilr3		+0.372	+0.707
ilr4		+0.089	-0.237
ilr5		+0.206	-0.188
ilr6		+0.046	-0.440
ilr1	P4	-0.394	+0.849
ilr2		+0.367	+0.489
ilr3		-0.026	+0.039
ilr4		+0.842	+0.186
ilr5		+0.003	+0.003
ilr6		-0.024	+0.061
ilr1	P5	+0.416	+0.826
ilr2		+0.071	+0.039
ilr3		-0.431	+0.453
ilr4		+0.035	+0.263
ilr5		+0.797	-0.201
ilr6		-0.022	+0.046

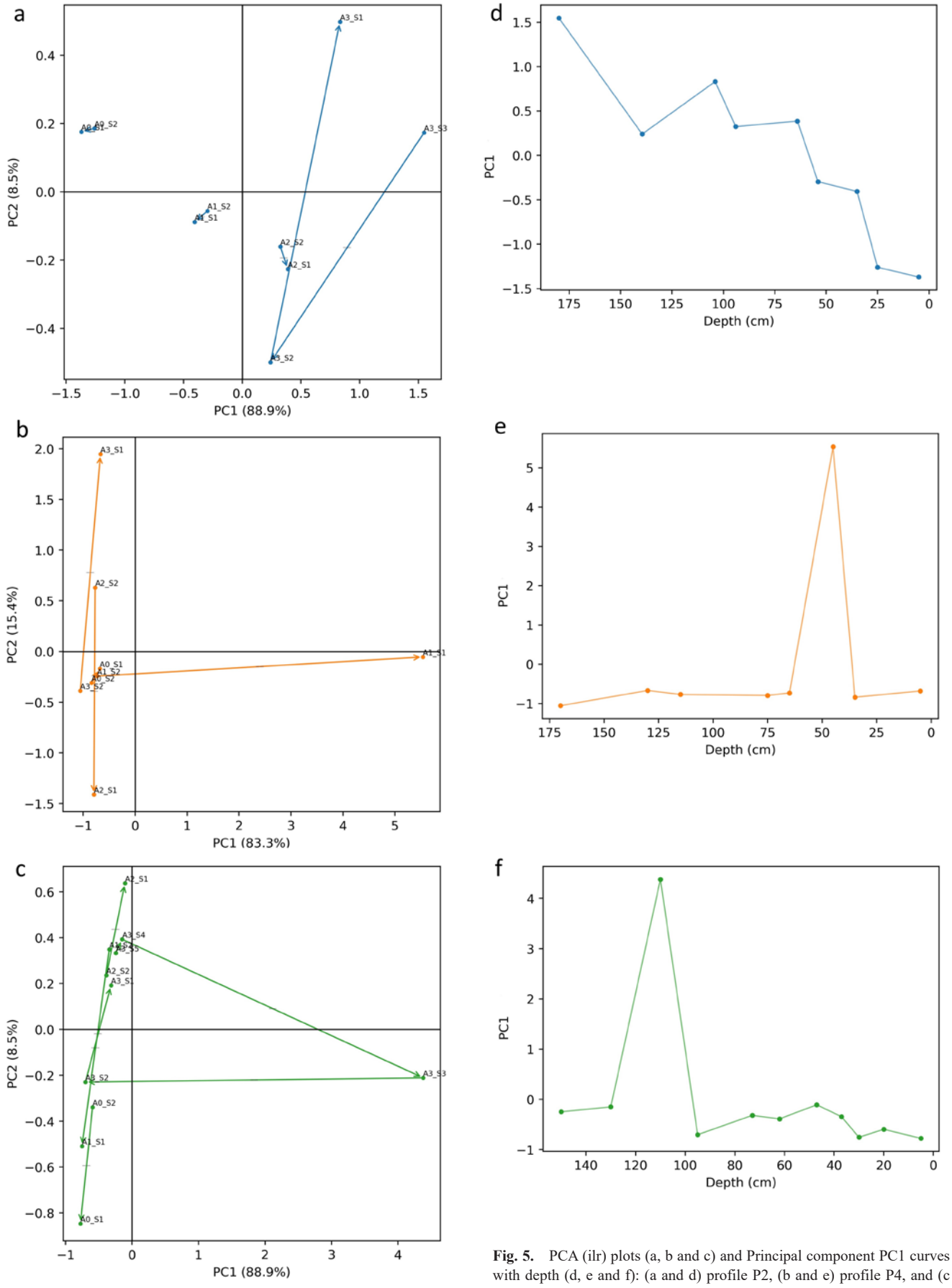

Fig. 5. PCA (ilr) plots (a, b and c) and Principal component PC1 curves with depth (d, e and f): (a and d) profile P2, (b and e) profile P4, and (c and f) profile P5.

Table 4. PCA scores (PC1 and PC2) for all samples.

Profile	Horizon	Sample	Depth_(cm)	PC1	PC2
P2	A0	S1	005.0	-1.370	+0.176
		S2	025.0	-1.260	+0.185
	A1	S1	035.0	-0.406	- 0.089
		S2	054.0	-0.296	- 0.056
	A2	S1	064.0	+0.387	- 0.226
		S2	094.0	+0.325	- 0.161
	A3	S1	104.5	+0.832	+0.497
		S2	139.5	+0.240	- 0.499
		S3	180.0	+1.548	+0.173
P4	A0	S1	005.0	-0.681	-0.170
		S2	035.0	-0.840	-0.310
	A1	S1	045.0	+5.539	-0.054
		S2	065.0	-0.732	-0.243
	A2	S1	075.0	-0.793	-1.412
		S2	115.0	-0.769	+0.631
	A3	S1	130.0	-0.668	+1.946
		S2	170.0	-1.056	-0.387
P5	A0	S1	005.0	-0.776	-0.847
		S2	020.0	-0.594	-0.340
	A1	S1	030.0	-0.754	-0.510
		S2	037.0	-0.345	+0.348
	A2	S1	047.0	-0.107	+0.637
		S2	062.0	-0.387	+0.236
	A3	S1	073.0	-0.318	+0.192
		S2	095.0	-0.702	-0.230
		S3	110.0	+4.378	-0.211
		S4	130.0	-0.149	+0.392
		S5	150.0	-0.247	+0.333

proportion of variance (8.5–15.4%) and captures secondary variability primarily associated with medium-sized fractions. This structure is consistent with ilr-based interpretations of granulometric balances, where PC1 reflects the fundamental coarse-fine sorting axis (Filzmoser *et al.*, 2009; Egozcue and Pawlowsky-Glahn, 2019) (Table 3), The ilr coordinates (ilr1–ilr6) correspond to the systolic blood pressure balances (B1–B6) specified in Table 2 and were calculated using Equation 1. Consequently, PC1 provides the most representative descriptor of vertical textural organization.

In profile P2 (Fig. 5a), deeper horizons (A3–A2) cluster at the coarse end of PC1, whereas surface horizons (A1–A0) plot toward finer compositions. The corresponding PC1–depth curve (Fig. 5d) shows a nearly monotonic fining upward trend, without abrupt discontinuities. PCA scores (Table 4) confirm gradual transitions between horizons.

Profile P4 exhibits a contrasting pattern (Fig. 5b). Although horizons remain aligned along PC1, the separation between A2 and A1_S1 is substantially larger than in P2. This is clearly expressed in the PC1-depth curve (Fig. 5e), which shows a pronounced inflection between 50 and 75 cm depth.

In profile P5 (Fig. 5c), most horizons plot at the fine end of PC1. The PC1-depth curve (Fig. 5f) displays a marked peak between 95 and 110 cm, corresponding to samples S3 and S4 for the horizon A3, which record high PC1 scores. the Table 4 includes two samples with high PC1 values, one in horizon A1 of profile P4 and one in horizon A3 of profile P5.

Ilr-PCA highlights a dominant vertical coarse-fine compositional gradient within each profile and reveals profile-specific differences in the magnitude and PSD variability with depth. Importantly. While ilr-PCA identifies the main axes of compositional variability and highlights vertical gradients within profiles, it does not quantify the magnitude of compositional change between successive horizons. To address this aspect, Aitchison distances and variation matrices were employed to assess the degree and internal structure of particle-size variability in the compositional space.

Some samples plot at one end of the PC1 axis, reflecting strong variations along the dominant compositional gradient from coarse to fine. These values are retained for descriptive purposes and do not affect the overall PCA structure or interpretation (Aitchison, 1986; Egozcue and Pawlowsky-Glahn, 2019).

Aitchison distance and variation matrix analysis

Aitchison distance and variation matrix analyses were used to quantify compositional dissimilarities between horizons and profiles, providing an integrated assessment of internal soil organization within the slope system. Distances between clr centroids of successive horizons were calculated to evaluate the magnitude of vertical compositional change (Fig. 6), following Aitchison (1982), Pawlowsky-Glahn and Buccianti (2011), and Pawlowsky-Glahn and Egozcue (2020). In profile P2, Aitchison distances range from 0.604 to 1.015, indicating relatively gradual compositional differences between successive horizons. Profile P4 exhibits the largest Aitchison distances among the three profiles, reflecting pronounced compositional contrasts between horizons. In profile P5, intermediate distance values

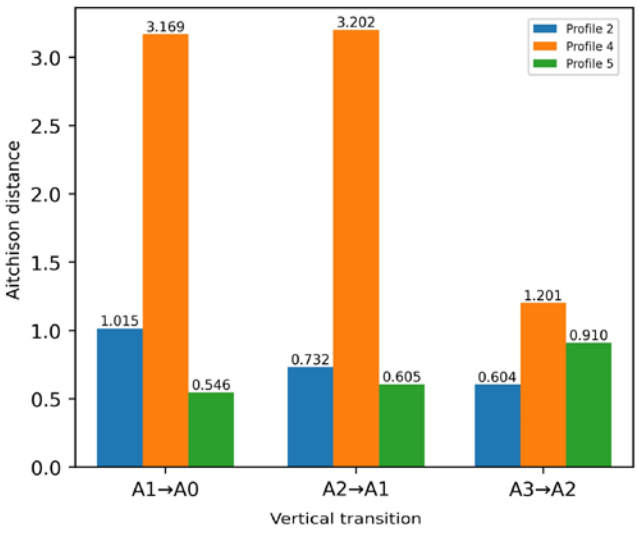

Fig. 6. Aitchison distances between successive horizons (A3→A2, A2→A1, A1→A0) for profiles P2, P4, and P5. This figure represents the Acheson distances between successive horizons for each cross profile, illustrating the relative magnitude of vertical compositional differences.

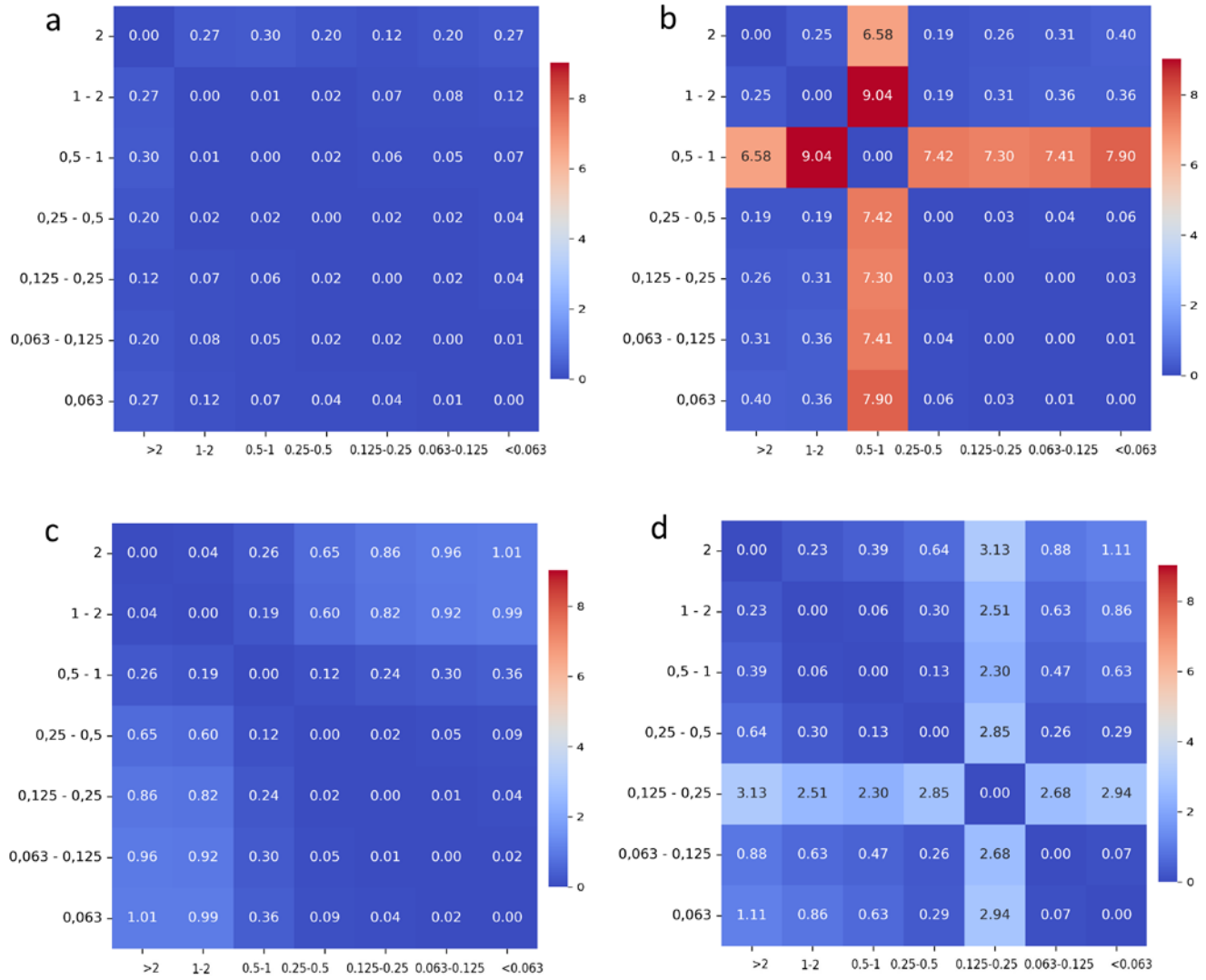

Fig. 7. Heatmaps of variation matrix for horizons, (a) horizon A0, (b) horizon A1, (c) horizon A2 and (d) horizon A3.

(0.546–0.910) are observed, with larger differences occurring primarily between deeper horizons.

Variation matrices were used to examine pairwise log-ratio variability among particle-size fractions within horizons (Fig. 7) and across profiles (Fig. 8). Horizon-level variation matrices show relatively low and uniform variance in horizon A0, whereas increased variability is observed in subsurface horizons, particularly involving medium and fine particle-size fractions. In deeper horizons (A3), variance is more evenly distributed across fractions.

Profile-level variation matrices reveal systematic lateral contrasts in compositional variability. Profile P2 displays generally low variance across particle-size fractions, whereas profile P4 exhibits localized zones of higher variance, indicating heterogeneous compositional relationships. Profile P5 shows lower overall variance, with narrow zones of elevated variability involving fine to medium fractions.

Aitchison distances and variation matrices document differences in the magnitude and structure of compositional variability both vertically within profiles and laterally along the slope.

End-Member Modelling Analysis (EMMA)

End-member modelling provides a quantitative framework for decomposing the observed granulometric variability into distinct sedimentary and pedogenic components. Four end-members were retained based on model performance and interpretability, consistent with established methodological recommendations (Weltje and Prins, 2003; Dietze M. and Dietze F., 2016).

The identified end-members represent distinct functional sedimentary domains. EM1 is dominated by very coarse sand and gravel. EM2 is characterized by coarse to medium sand fractions. EM3 and EM4 are enriched in fine and very fine fractions (fine sand, silt, and clay).

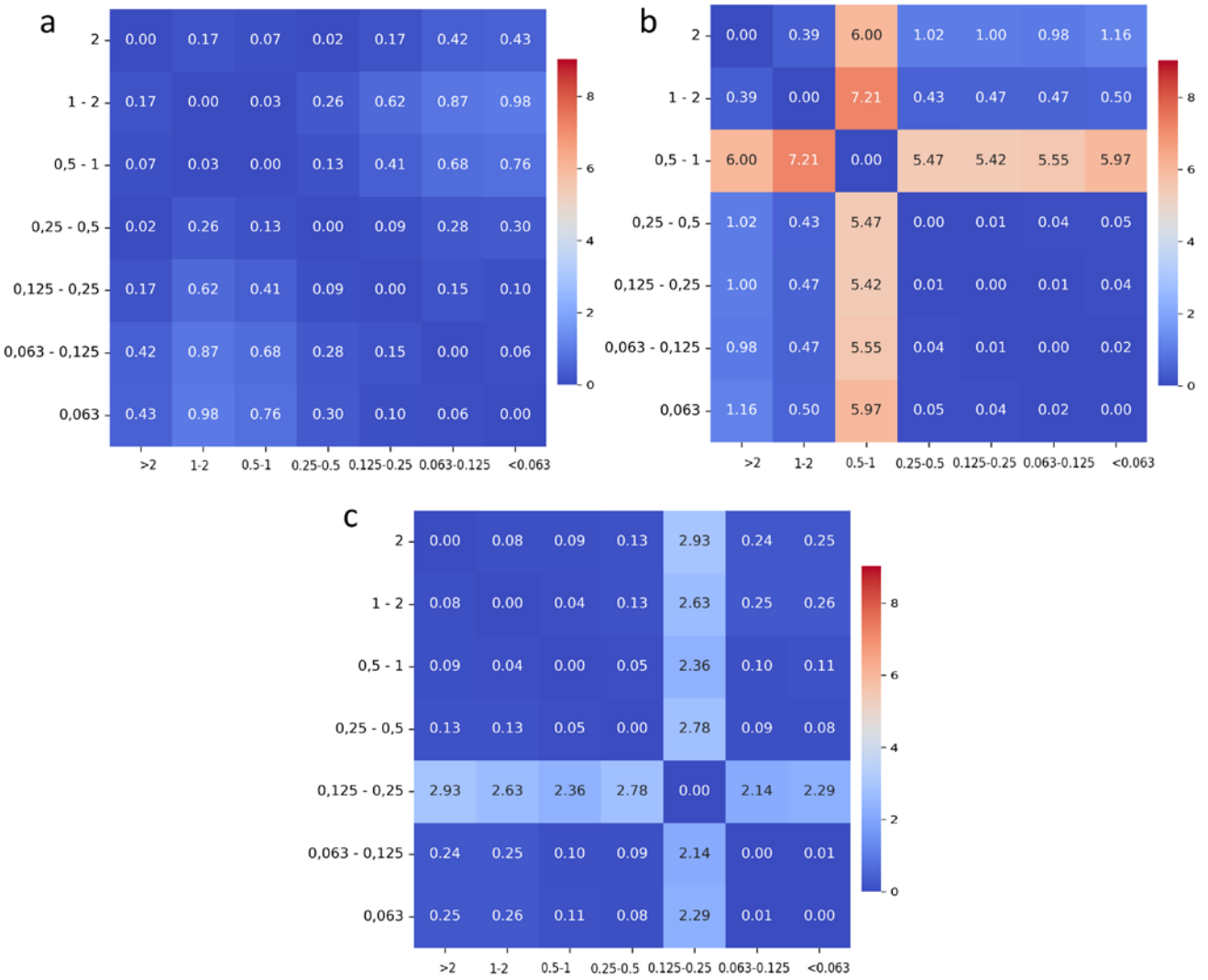

Fig. 8. Heatmaps of variation matrix for profiles, (a) profile P2, (b) profile P4, and (c) profile P5.

Vertical mixing along profiles

End-member proportions vary systematically with depth and slope position (Fig. 9). In profile P2, EM1 dominates throughout the profile with limited vertical variability. A modest increase in EM4 near the surface reflects an enrichment of fines in A0–A1 horizons. Profile P4 exhibits alternating dominance of EM1, EM3, and EM4, indicating heterogeneous vertical mixing of particle-size assemblages. In Profile P5, EM3 dominates deeper horizons, while EM4 increases toward the surface, producing a clear fining-upward trend.

Lateral variability along the slope

The stacked end-member distributions (Fig. 10) highlight systematic lateral trends. Profile P2 is consistently dominated by EM1>50%. Profile P4 shows mixed contributions from all end-members. Profile P5 is dominated by EM3 and EM4 (>70%).

These lateral patterns illustrate particle-size fractionation controlled by the transition from erosional domains upslope to depositional environments downslope. The results are consistent with classical slope sediment dynamics (Kirkby, 1971; Holliday *et al.*, 2008) and recent EMMA applications in semi-arid soil systems (Dietze *et al.*, 2014).

The EMMA results identify a limited number of statistically coherent particle-size assemblages whose vertical and lateral distributions vary systematically between profiles.

DISCUSSION

The integrated application for compositional data analysis, multivariate statistics, and end-member modelling provides a coherent framework for interpreting vertical and

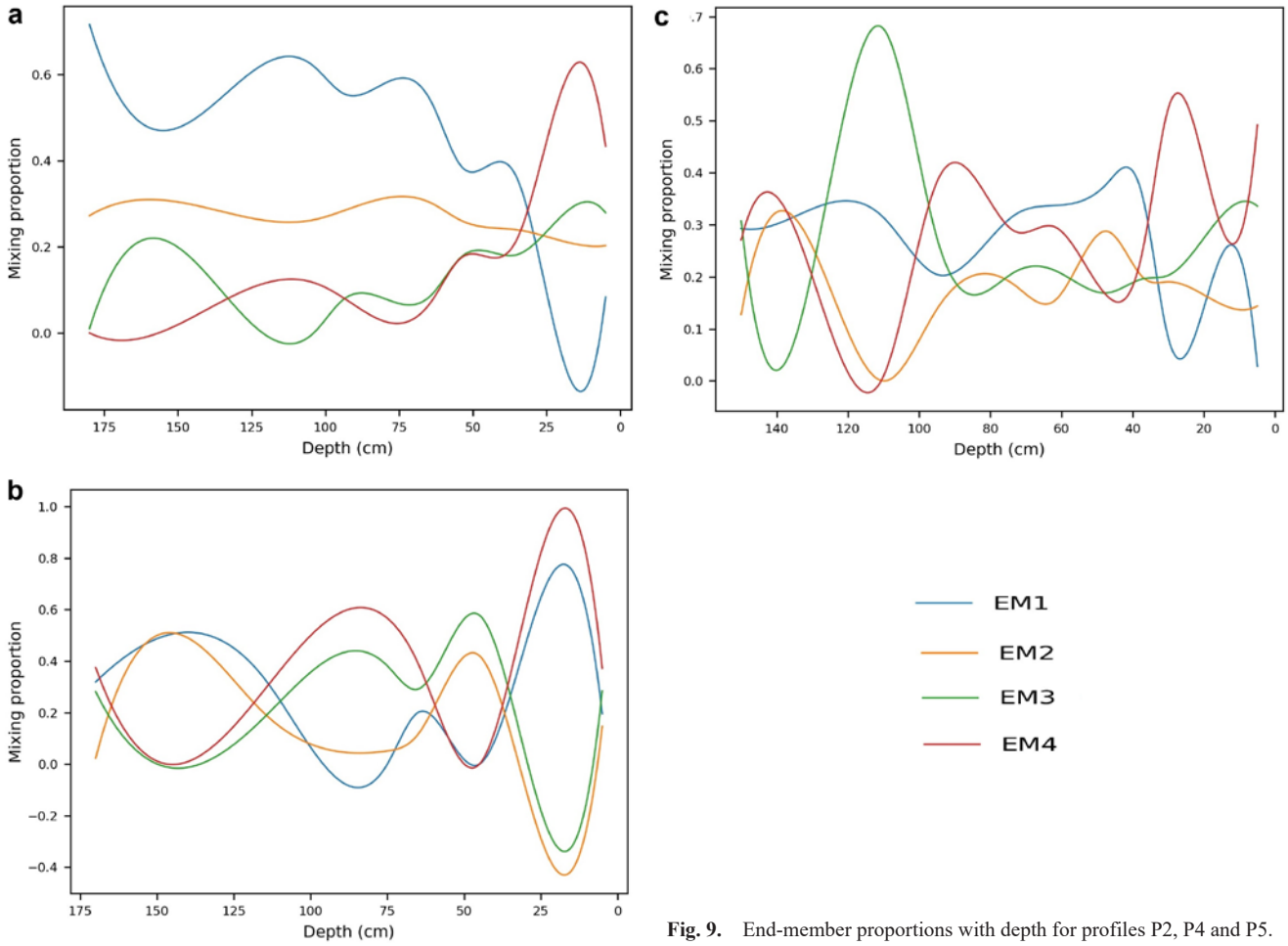

Fig. 9. End-member proportions with depth for profiles P2, P4 and P5.

lateral patterns of particle-size distributions (PSD) along the studied agricultural hillslope. By taking into account the compositional nature of particle-size data, this approach allows for a comparison of particle-size variation across horizons and locations on the hillslope, while avoiding the biases associated with traditional analyses of closed data sets (Aitchison, 1986; Filzmoser *et al.*, 2009; Zhang and Shi, 2020).

In all profiles, compositional and multivariate analyses consistently identify a dominant coarse-fine gradient, which is clearly evident in the first principal component PC1. This gradient reflects relative changes in PSD with depth and along the hillslope, but should be understood as a descriptive statistical structure than a direct indicator of pedogenetic or sedimentary processes. In the upslope profile P2, limited internal variation and vertical trends indicate a relatively stable particle organisation, consistent with weak lateral redistribution due to its proximity to the parent material. Similar patterns have been described for upslope locations where PSD with limited sediment inputs and removals (FitzPatrick, 1983; Jenny, 1941, 1980). The midslope profile (P4) shows clear vertical heterogeneity, reflected by abrupt shifts in PCA scores and elevated Aitchison distances between successive horizons. Such patterns are characteristic of geomorphically active midslope environments, where sediment supply and transport capacity fluctuate over time (Sommer and Schlichting, 1997; Van Oost *et al.*, 2006; Mudd and Furbish, 2007). The observed textural contrasts therefore indicate enhanced compositional variability rather than steady vertical differentiation. In th downslope (P5), enrichment in fine fractions is consistent with effective accumulation and retention of finer material. as transport downslope enhances the concentration of fine particles in the deeper horizons (Kosmas *et al.*, 2000; Schmengler, 2011; Sklar *et al.*, 2017). However, because all materials smaller than 0.063 mm are concentrated in one fraction, explanations involving fine soil formation mechanisms remain conditional and unspecified. Vertical variation in soil texture within profiles may result from a combination of inherited material properties, gradual soil development, and post-depositional reorganisation, particularly in cultivated areas where PSD may change in the horizons. Variation matrices indicate horizon and profile levels textural organisation. Surface horizons are homogenised by cultivation, whereas subsurface horizons show selective sorting linked to parent material influence and limited pedogenic differentiation (Hartmann *et al.*, 2020). Along the slope, textural variability decreases downslope, reflecting transport controlled fine and sorting particles accumulation (Zadorova *et al.*, 2023; Luo *et al.*, 2024).

End-member modelling highlights clear vertical and lateral variations in particle-size organisation along the

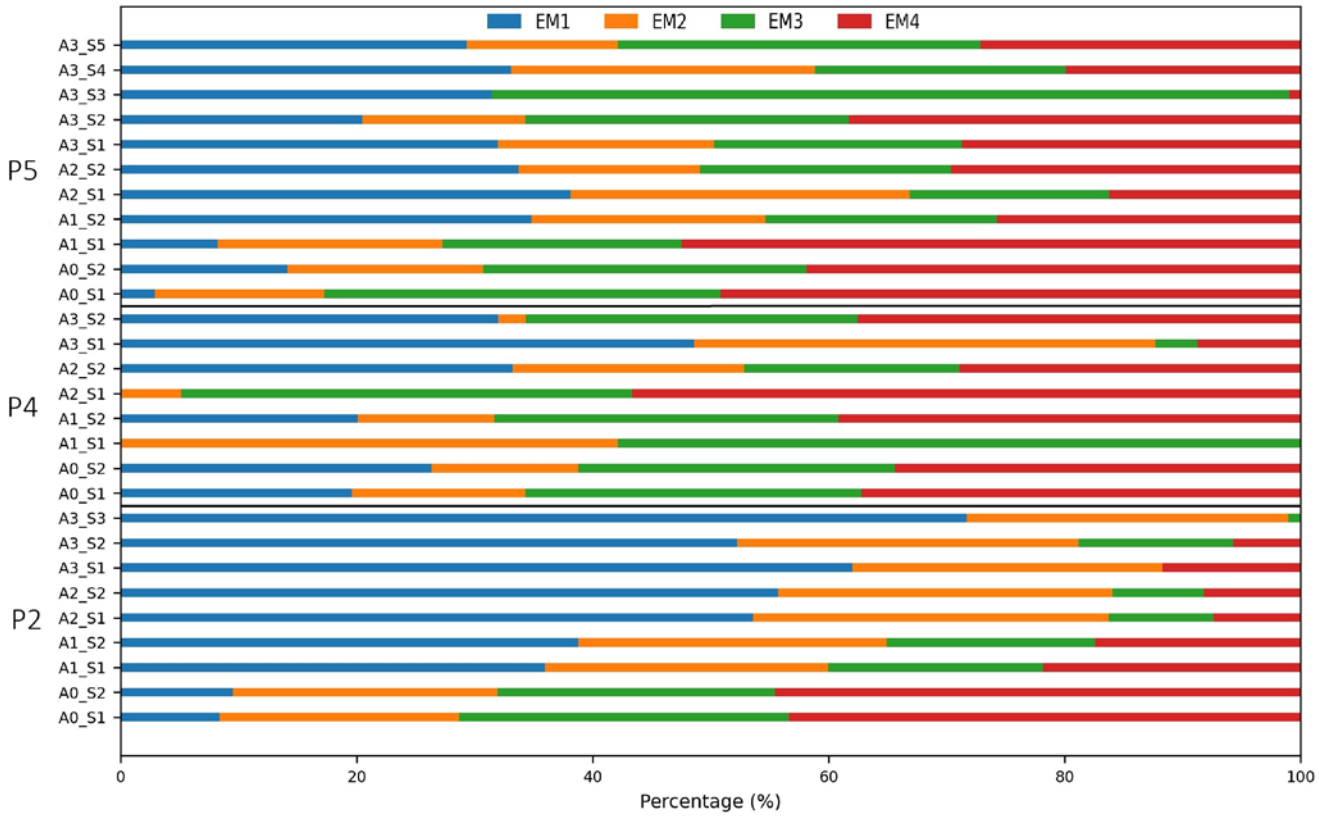

Fig. 10. Stacked barplot of end-member percentages per sample grouped in each profile.

hillslope. The dominance of coarse-grained assemblages (EM1) at upslope, the mixed contributions (EM3–EM4) at midslope, and the prevalence of fine-grained assemblages downslope reflect systematic textural organisation associated with the morphology of the area. Such gradients reflect particle-size fractionation controlled by transport efficiency and slope geometry, consistent with conceptual erosion-deposition models and recent EMMA applications in soil systems (Dietze *et al.*, 2014, 2022).

The convergent patterns revealed by clr-transformed heatmaps, principal component analysis (PCA), variation matrices, and end-member modelling analysis (EMMA), indicate a clear textural gradient along the hillslope. In profile P2, where the soil profile is located close to the parent rock that constitutes the primary source of materials, relatively homogeneous particle-size assemblages dominated by coarse fractions prevail, reflecting limited transport and a strong lithological control. In profile P4 display, there is an abundance and heterogeneity of PSDs. The downslope profile P5 shows a marked enrichment in fine fractions. Where geomorphological conditions, particularly slope gradient and proximity to the watercourse-promote particles transport by surface runoff. This organisation corresponds to the slope gradient, particle sorting and redistribution driven by hydrodynamic and topographic. The coherence between field observations and the results of multivariate compositional and statistical analyses supports this interpretation and is consistent with classical conceptual models of soil evolution along hillslopes (Quine *et al.*, 1997; Egli *et al.*, 2008).

Since this study is based on three soil sections located along a single agricultural hillslope, the interpretations presented here should be considered specific to this area. Extrapolation these patterns to other agricultural hillslopes would require additional spatial replication and comparative datasets.

CONCLUSIONS

This study provides a focused assessment of vertical and lateral soil PSD along an agricultural hillslope at Mechtat Kef Laatatfa (Ouled Hamla, northeastern Algeria), using an integrated compositional and multivariate analytical framework. By jointly applying CoDA, PCA, and EMMA, the study demonstrates the relevance of compositional approaches for analysing soil granulometry while accounting for the closed nature of particle-size data.

The results reveal a coherent downslope organisation of soil texture, characterised by coarse, parent-material-dominated soils in upslope positions, a texturally heterogeneous and actively reworked midslope zone, and fine-enriched, relatively stable soils at the slope base. This systematic pattern highlights hillslope position as a primary control on PSD structuring and sediment redistribution within the studied agricultural landscape.

A key contribution of this work lies in the combined use of CoDA and EMMA for soil particle-size analysis. This integration enables a more refined characterisation of fineness gradients, internal structural variability, and transport-related sorting processes that are not readily captured by conventional texture indices. Treating particle-size fractions explicitly as compositional data within the Aitchison geometry reduces statistical artefacts associated with closure and allows granulometric variability to be interpreted in a physically meaningful way. When coupled with PCA and end-member modelling, this framework enhances sensitivity to subtle textural changes and strengthens the linkage between statistical patterns and geomorphological processes.

From an applied perspective, the findings contribute to a better understanding of soil structural variability and its relationship with hillslope characteristics, with direct implications for assessing erosion susceptibility, guiding soil management practices, and informing land-use planning on cultivated slopes. While the exclusive use of dry sieving and the aggregation of fractions finer than 0.063 mm limit detailed interpretation of pedogenetic processes, the observed patterns remain robust at the hillslope scale and consistent with the identified sediment redistribution mechanisms.

Future research should integrate mineralogical and geochemical tracers, hydrological measurements, and temporal monitoring to further constrain sediment sources, quantify transport dynamics, and evaluate the persistence of PSD patterns over time. Such extensions would strengthen process-based interpretations and broaden the applicability of compositional frameworks in hillslope soil and geomorphological studies.

REFERENCES

Aitchison, J., 1982. The statistical analysis of compositional data. Journal of the Royal Statistical Society: Series B (Methodological) 44(2), 139–160.

Aitchison, J., 1983. Principal component analysis of compositional data. Biometrika 70 (1), 57–65.

Aitchison, J., 1986. The statistical analysis of compositional data, Chapman and Hall, Ltd., pp. 416.

Aitchison, J., Greenacre, M., 2002. Biplots for compositional data. Journal of the Royal Statistical Society Series C: Applied Statistics 51(4), 375–392.

Anderson, R.S., Anderson, S.P., 2010. Geomorphology: the mechanics and chemistry of landscapes. Cambridge University Press.

Arif, I., Hadji, R., Hamed, Y., Hamdi, N., Gentilucci, M., Hajji, S., 2024. Geoenvironmental factors influencing slope failures in the Majerda Basin at the Algerian–Tunisian border. Euro-Mediterranean Journal for Environmental Integration 9(1), 355–376.

Aris, Y., 1994. Études tectonique et microtectonique des séries jurassiques à plio-quaternaires du constantinois central (Algérie Nord-Orientale): caractérisation des différentes phases de déformation. Thèse de Doctorat de l'université Nancy I, p.

Bär, C.B., 1957. Etude géologique de la feuille au 1/50.000 e d'Ain M'lila (Algérie). Service de la carte géologique de l'Algérie. Alger. Bulletin 9, p. 249.

Benmarce, K., Hadji, R., Hamed, Y., Zahri, F., Zighmi, K., Hamad, A., Gentilucci, M., 2023. Hydrogeological and water quality analysis of thermal springs in the Guelma region of northeastern Algeria using hydrochemical, statistical, and isotopic approaches. Journal of African Earth Sciences 205, Article 105011.

Bouillin, J.P., 1986. Le» bassin maghrebin»; une ancienne limite entre l'Europe et l'Afrique a l'ouest des Alpes. Bulletin de la Société géologique de France 2(4), 547–558.

Buccianti, A., 2013. Is compositional data analysis a way to see beyond the illusion? Computers & geosciences 50, 165–173.

Buol, S.W., Southard, R.J., Graham, R.C., McDaniel, P.A., 2011. Soil genesis and classification. John Wiley & Sons.

Bureau, D., 1986. Approche sédimentaire de la dynamique structurale: évolution mésozoïque et devenir orogénique de la partie septentrionale du fossé saharien (Sud-Ouest constantinois et Aurès, Algérie). Thèse d'Etat. Univ. Pierre et Marie Curie, Paris VI, 441P (.

Canfield, H.E., Lopes, V.L., Goodrich, D.C., 2001. Hillslope characteristics and particle size composition of surficial armoring on a semiarid watershed in the southwestern United States. Catena 44(1), 1–11.

Chadi, M., 1991. Géologie structurale des monts d'Aïn M'Lila (Algérie orientale) (Doctoral dissertation, Nancy 1).

Chadi, M., 2004. Cadre géologique et structural des séries néritiques du constantinois (Est Algérien). Thèse de doctorat d'Etat. Univ. Mentouri Constantine, p. 229.

Chen, Z.S., Hsieh, C.F., Jiang, F.Y., Hsieh, T.H., Sun, I.F., 1997. Relations of soil properties to topography and vegetation in a subtropical rain forest in southern Taiwan. Plant Ecology 132, 229–241.

Chi, Z., Xu, X.-Y., Liu, K.-L., Liu, H.-J., Meng, R.-L., Li, Y.-Q., Fu, L., Li, X.-N., 2021. Study on soil particle size characteristics and spatial pattern of sand deposition in two types of sand barriers. Journal of Soil and Water Conservation 35(2), 113–121

Chibani, A., Hadji, R., Hamed, Y., Gentilucci, M., Shuhab, K., Khalil, R., Asghar, B., 2024. Hydrogeological characterization of a multilayer aquifer system in the Tunisian–Algerian border region using geological and geophysical techniques. Earth Systems and Environment 9(2), 1165–1190.

Coiffait, P.E., 1992. Un bassin post-nappes dans son cadre structural : l'exemple du bassin de Constantine (Algérie nord-orientale) (Doctoral dissertation, Nancy 1).

Dahoua, L., Yakovitch, S.V., Hadji, R., Farid, Z., 2017. Landslide susceptibility mapping using the analytic hierarchy process: Case study of the East-West Highway in the BBA-Bouira region, northeastern Algeria. In : Proceedings of the Euro-Mediterranean Conference for Environmental Integration, 1837–1840.

Dietze, E., Hartmann, K., Diekmann, B., Imker, J., Lehmkuhl, F., Opitz, S., Borchers, A., 2012. An end member algorithm for deciphering modern detrital processes from lake sediments of Lake Donggi Cona, NE Tibetan Plateau, China. Sedimentary Geology 243–244, 169–180.

Dietze, E., Maussion, F., Ahlborn, M., Diekmann, B., Hartmann, K., Henkel, K., Haberzettl, T., 2014. Sediment transport processes across the Tibetan Plateau inferred from robust grain-size end members in lake sediments. Climate of the Past 10, 191–106.

Dietze, M., Dietze, E., 2016. EMMAgeo: End-member modelling of grain-size data [Computer software manual]. R Package Version 0.9.6.

Dietze, M., Schulte, P., Dietze, E., 2022. Application of end-member modelling to grain-size data: Constraints and limitations. Sedimentology 69(2), 845–863.

Durozoy, G., 1960. Reconnaissance géologique dans le Hank (Sahara occidental). Publication du Service de la Carte Géologique de l'Algérie, Bulletine 28, 21–42.

Egli, M., Mirabella, A., Sartori, G., 2008. The role of climate and vegetation in weathering and clay mineral formation in late Quaternary soils of the Swiss and Italian Alps. Geomorphology 102(3–4), 307–324.

Egozcue, J.J., Pawlowsky-Glahn, V., 2005. Groups of parts and their balances in compositional data analysis. Mathematical Geology 37(7), 795–828.

Egozcue, J.J., Pawlowsky-Glahn, V., 2019. Compositional data: the sample space and its structure. TEST 28(3), 599–638.

Egozcue, J.J., Pawlowsky-Glahn, V., Mateu-Figueras, G., Barcelo-Vidal, C., 2003. Isometric logratio transformations for compositional data analysis. Mathematical Geology 35, 279–300.

Filzmoser, P., Hron, K., 2009. Correlation analysis for compositional data. Mathematical Geosciences 41, 905–919.

Filzmoser, P., Hron, K., Reimann, C., 2009. Principal component analysis for compositional data with outliers. Environmetrics: The Official Journal of the International Environmetrics Society 20(6), 621–632.

FitzPatrick, E.A., 1983. Soils Their formation classification and distribution Longman Scientific and Technical.

Flemming, B.W., 2007. The influence of grain-size analysis methods and sediment mixing on curve shapes and textural parameters: Implications for sediment trend analysis. Sedimentery Geology 202, 425–435.

Folk, R.L., Ward, W.C., 1957. Brazos River bar [Texas]; a study in the significance of grain size parameters. Journal of Sedimentary Research 27(1), 3–26.

Guiraud, R., 1990. Evolution Post-Triasique de l'avant pays de la chaine alpine en Algérie d'après l'étude du Bassin de Hodna et des régions voisines. Mémoire 3, Service Géologique de l'Algérie. Alger, 271p, 114 fig., XII pl. h.t.

Hamed, Y., Hadji, R., Ahmadi, R., Ayadi, Y., Shuhab, K., Pulido-Bosch, A., 2024. Hydrogeological investigation of karst aquifers using integrated geomorphological, geochemical, GIS, and remote sensing techniques in the southern Mediterranean Basin (Tunisia). Environment, Development and Sustainability 26(3), 6943–6975.

Han, M., Guo, Y., Zhang, C., Qi, W., Cheng, L., Feng, Y., Song, Y., Yang, W., 2025. Multivariate analysis of soil particle size distribution and Spatial correlation with soil moisture characteristics in different vegetation types of Mu Us Sandy Land. Scientific Reports 15(1), Article 25659.

Hartmann, A., Weiler, M., Blume, T., 2020. The impact of landscape evolution on soil physics: Evolution of soil physical and hydraulic properties along two chronosequences of proglacial moraines. Earth System Science Data 12(4), 3189–3204.

Holliday, V.T., McFadden, L.D., Bettis, E.A., Birkeland, P.W., 2008. Soil survey and soil geomorphology. Profiles in the History of the US Soil Survey, 233.

Hosseinpoor, M.J., Moini, H., Torab, F.M., 2015. Detecting and mapping compositional global outliers to identify mineral exploration targets, Case study: Khusf district, East of Iran. In: Thió-Henestrosa, S., Martín Fernández, J.A. (Eds), Proceedings of the 6th International Workshop on Compositional Data Analysis, CoDaWork, 175–186.

Jenny, H., 1941. Factors of Soil Formation: A System of Quantitative Pedology. McGraw-Hill, New York, pp. 281.

Jenny, H., 1980. The Soil Resource: Origin and Behaviour. Ecological Studies 37. Springer, New York, pp. 377.

Kazi-Tani, N., 1986. Evolution géodynamique de la bordure nord-Africaine (Doctoral dissertation, Bordeaux).

Kirkby, M.J., 1971. Hillslope process-response models based on the continuity equation. Institute of British Geographers Special Publication 3(1), 5–30.

Kosmas, C., Gerontidis, S., Marathianou, M., 2000. The effect of land use change on soils and vegetation over various lithological formations on Lesvos (Greece). Catena 40(1), 51–68.

Ladjel, Z., Zahri, F., Hadji, R., Hamed, Y., Zighmi, K., Benmarce, K., 2024. Integrated hazard assessment of rockfall incidents in the Cap Aokas cliff region. Journal of Mountain Science 21(6), 1916–1929.

Lahondère, J.C., 1987. Les séries ultratelliennes d'Algérie nord-orientale et les formations environnantes dans leur cadre structural (Doctoral dissertation, Toulouse).

Luo, B., Li, J., Tang, J., Wei, C., Zhong, S., 2024. Microtopography effects on pedogenesis in the mudstone-derived soils of the hilly mountainous regions. Scientific Reports 14(1), Article 11998.

Martín-Fernandez, J.A., Barcelol Vidal C., Pawlowsky-Glahn, V., 2003. Dealing with zeros and missing values in compositional data sets using nonparametric imputation. Mathematical Geology 35, 253–278.

McKenzie, N.J., Ryan, P.J., 1999. Spatial prediction of soil properties using environmental correlation. Geoderma 89, 67–94.

Mudd, S.M., Furbish, D.J., 2007. Responses of soil-mantled hillslopes to transient channel incision rates. Journal of Geophysical Research: Earth Surface 112, Article F03S18.

Ncibi, K., Mastrocicco, M., Colombani, N., Busico, G., Hadji, R., Hamed, Y., Shuhab, K., 2022. Differentiating nitrate origins and fate in a semi-arid basin (Tunisia) using geostatistical analyses and groundwater modelling. Water 14(24), Article 4124.

Obert, D. 1974. Phases tectoniques mesozoiques d'age ante-cenomanien dans les Babors (Tell nord-setifien, Algerie). Bulletin de la Société géologique de France 7(2), 171–176.

Pawlowsky-Glahn, V., Buccianti, A., 2011. Compositional Data Analysis: Theory and Applications. John Wiley & Sons, pp. 378.

Pawlowsky-Glahn, V., Egozcue, J.J., 2006. Compositional data and their analysis: an introduction. Geological Society, London, Special Publications 264(1), 1–10.

Pawlowsky-Glahn, V., Egozcue, J.J., 2020. Compositional data in geostatistics: A log-ratio based framework to analyze regionalized compositions. Mathematical Geosciences 52(8), 1067–1084.

Quine, T.A., Govers, G., Walling, D.E., Zhang, X., Desmet, P.J., Zhang, Y., Vandaele, K., 1997. Erosion processes and landform evolution on agricultural land—new perspectives from caesium-137 measurements and topographic-based erosion modelling. Earth Surface Processes and Landforms: The Journal of the British Geomorphological Group 22(9), 799–816.

Raoult, J.F., Fourcade, E., 1973. Sur le Crétacé inférieur du Djebel Friktia (Môle Néritique Constantinois, Algérie). Compte Rendu Sommaire de la Société Géologique de France, Paris, 369–370.

Saadoun, A., Fredj, M., Boukarm, R., Hadji, R., 2022. Fragmentation analysis using digital image processing and the empirical Kuz-Ram model: A comparative study. Zapiski Gornogo Instituta 257, 822–832.

Schaetzl, R.J., Anderson, S., 2005. Soils: Genesis and geomorphology. Cambridge University Press.

Schmengler, A.C., 2011. Modeling soil erosion and reservoir sedimentation at hillslope and catchment scale in semi-arid Burkina Faso (Doctoral dissertation, Universitäts-und Landesbibliothek Bonn).

Singh, M.C., Satpute, S., Prasad, V., 2023. Remote sensing and GIS-based watershed prioritization for land and water conservation planning and management. Water Science & Technology 88(1), 233–265.

Sklar, L.S., Riebe, C.S., Marshall, J.A., Genetti, J., Leclere, S., Lukens, C.L., Merces, V., 2017. The problem of predicting the size distribution of sediment supplied by hillslopes to rivers. Geomorphology 277, 31–49.

Sommer, M., Schlichting, E., 1997. Archetypes of catenas in respect to matter—a concept for structuring and grouping catenas. Geoderma 76(1–2), 1–33.

Syms, C., 2008. Principal components analysis. In: Jørgensen, S.E., Fath, B.D. (Eds), Encyclopedia of Ecology, Elsevier, pp. 2940–2949.

Taib, H., Hadji, R., Hamed, Y., Bensalem, M.S., Amamria, S., 2024a. Exploring neotectonic activity in a semiarid basin: A case study of the Ain Zerga watershed. Journal of Umm Al-Qura University for Applied Sciences 10(1), 20–33.

Taib, H., Hadji, R., Hamed, Y., Bensalem, M.S., Amamria, S., Houda, B., 2024b. Evaluation of relative tectonic activity in a semiarid basin using geomorphic indices and morphometric parameters: The Meskiana watershed. Euro-Mediterranean Journal for Environmental Integration 9(2), 843–858.

Tancredi, M.T., Gaur, N., Markewitz, D., Levi, M.R., 2022. Determination of high-resolution soil texture profile at the hillslope scale. Geoderma 428, Article 116189.

Van de Fliert, J.R., 1955. Etude géologique de la region d'oued el Athmenia (Algérie). Service de la carte géologique de l'Algérie, Alger. Bulletin 3, p. 264.

Van Hateren, J.A., Prins, M.A., Van Balen, R.T., 2018. On the genetically meaningful decomposition of grain-size distributions: A comparison of different end-member modelling algorithms. Sedimentary Geology 375, 49–71.

Van Oost, K., Govers, G., De Alba, S., Quine, T.A., 2006. Tillage erosion: a review of controlling factors and implications for soil quality. Progress in Physical Geography 30(4), 443–466.

Vandenberghe, J., 2013. Grain size of fine-grained windblown sediment: A powerful proxy for process identification. Earth-Science Reviews 121, 18–30.

Vila, J.M., 1980. La chaîne alpine d'Algérie orientale et des confins Algéro-tunisiens. Thèse de Doctorat ès-Sciences, Paris VI, 2 t., p. 665.

Voute, C., 1967. Synthesis of the geological history of the Ain Fakroun-Ain Babouche area and surrounding regions. Detailed description of the Ain Fakroun and Ain Babouche sheets of the 1:50,000 geological map.

Wang, N., Eziz, M., Mao, D., Sidekjan, N., 2023. Fractal characteristics of the particle size distribution of soil along an urban-suburban-rural-desert gradient. Land 12(12), Article 2120.

Weltje, G.J., Prins, M.A., 2003. Muddled or mixed? Inferring palaeoclimate from size distributions of deep-sea clastics. Sedimentary Geology 162(1–2), 39–62.

Zadorova, T., Penížek, V., Koubova, M., Lisá, L., Pavlů, L., Tejnecký, V., ..., Kodešová, R., 2023. Formation of Colluvisols in different soil regions and slope positions (Czechia): Post-sedimentary pedogenesis in colluvial material. Catena 229, Article 107233.

Zhang, M., Shi, W., 2020. Compositional balance should be considered in soil particle-size fractions mapping using hybrid interpolators. Hydrology and Earth System Sciences Discussions, hess-2020–384. https://doi.org/10.5194/hess-2020-384, 2020

Zerzour, O., Gadri, L., Hadji, R., Mebrouk, F., Hamed, Y., 2020. Semi-variograms and kriging techniques in iron ore reserve categorization: Application to the Jebel Wenza deposit. Arabian Journal of Geosciences 13(16), Article 820.

Zerzour, O., Gadri, L., Hadji, R., Mebrouk, F., Hamed, Y., 2021. A geostatistics-based method for irregular mineral resource estimation: Application to the Ouenza iron mine, northeastern Algeria. Geotechnical and Geological Engineering 39(5), 3337–3346.